

An effective field theory analysis of Efimov physics in heteronuclear mixtures of ultracold atomic gases

Bijaya Acharya,^{1,*} Chen Ji,^{2,3,4,†} and Lucas Platter^{1,5,‡}

¹*Department of Physics and Astronomy,*

University of Tennessee, Knoxville, TN 37996, USA

²*ECT*, Villa Tambosi, 38123 Villazzano (Trento), Italy*

³*INFN-TIFPA, Trento Institute for Fundamental Physics and Applications, Trento, Italy*

⁴*TRIUMF, 4004 Wesbrook Mall, Vancouver, BC V6T 2A3, Canada*

⁵*Physics Division, Oak Ridge National Laboratory, Oak Ridge, TN 37831, USA*

(Dated: May 22, 2022)

Abstract

We use an effective field theory framework to analyze the Efimov effect in heteronuclear three-body systems consisting of two species of atoms with a large interspecies scattering length. In the leading-order description of this theory, various three-body observables in heteronuclear mixtures can be universally parameterized by one three-body parameter. We present the next-to-leading corrections, which include the effects of the finite interspecies effective range and the finite intraspecies scattering length, to various three-body observables. We show that only one additional three-body parameter is required to render the theory predictive at this order. By including the effective range and intraspecies scattering length corrections, we derive a set of universal relations that connect the different Efimov features near the interspecies Feshbach resonance. Furthermore, we show that these relations can be interpreted in terms of the running of the three-body counterterms that naturally emerge from proper renormalization. Finally, we make predictions for recombination observables of a number of atomic systems that are of experimental interest.

*Electronic address: bacharya@utk.edu

†Electronic address: ji@ectstar.eu

‡Electronic address: lplatter@utk.edu

I. INTRODUCTION

Three-body systems of identical bosons display the Efimov effect [1] when the interatomic scattering length is much larger than the range of the underlying interaction. The key signature of the Efimov effect is the discrete scaling of observables. For example, in the limit of infinitely large scattering length, the three-body bound state energies are in a geometric progression with a common ratio λ^2 , where the scaling factor λ has the value 22.694 for a system of three identical bosons [2]. Multiple experiments with ultracold atomic gases consisting of identical bosons have found signatures of the Efimov effect by measuring loss rates that are driven by three-body recombination effects in these systems [3–6]. The Efimov effect also exists for systems of distinguishable particles with different mass ratios. This motivated for example the first experimental measurement in heteronuclear atomic systems by the Florence group [7] and more recent experiments with Lithium-Cesium mixtures [8, 9]. Such systems also exist in nuclear physics as neutron-rich halo nuclei, which are weakly bound nuclei consisting of a tightly bound core and a small number of valence neutrons [10, 11].

The discrete scaling invariance and other scaling laws among Efimov features in heteronuclear three-body systems have been calculated in the zero-range limit by Helfrich *et al.* [12] using an effective field theory framework. Various potential models, such as a minimal zero-range model [13] and Lennard-Jones potentials (with van der Waals tails) [14], have also investigated the Efimov physics in heteronuclear systems. These theoretical works found better agreement with experimental results for shallower Efimov states but stronger discrepancies for deeper states. Such discrepancies are expected to be associated with the finite effective ranges. It is therefore important to understand the range corrections in a systematic framework.

Effective field theory (EFT) has been shown to be a convenient tool to estimate uncertainties related to higher-order corrections in a model-independent manner. EFTs are based on a systematic low-energy expansion in a small parameter that is formed by a ratio of two separated scales inherent to the problem at hand. In systems that display the Efimov effect, this parameter is the ratio of the range of the interaction to the scattering length.

The so-called *short-range* EFT at leading order (LO) has been used extensively to describe the zero-range limit of atoms interacting through a large scattering length. Finite effective

range corrections were first considered within this framework in Ref. [15]. However, nuclear systems with a fixed scattering length were considered in this work. In Refs. [16, 17], the effective range, r_0 , was included for the case of variable scattering length and it was found that within the EFT a second three-body datum is required for the approach to be predictive at this order.

An additional complication arises in heteronuclear three-body systems because there are two different scattering lengths. Near the interspecies Feshbach resonance, the two identical atoms interact with each other through a smaller scattering length leading to deviations from the scaling laws.

In this paper, we consider a three-body system of two identical bosons (denoted by 2) that interact with one distinguishable atom (denoted by 1) via a large s -wave interspecies scattering length a_{12} and a small intraspecies scattering length a_{22} . Such a system could for example be prepared by choosing an appropriate Feshbach resonance in the Lithium-Cesium system [8, 9]¹. We study low-energy processes that occur at a typical momentum $k \sim a_{12}^{-1}$ by expressing all observables as simultaneous expansions in kr_0 and ka_{22} . At LO in this expansion, we recover the results obtained by Helfrich *et al.* [12]. We work to next-to-leading order (NLO) where corrections linear in r_0/a_{12} and a_{22}/a_{12} enter. We show that these corrections can be interpreted in terms of the renormalization group of the EFT [18]. We then propose analytic formulas that account for the higher order corrections in a simple manner.

II. EFFECTIVE FIELD THEORY

In terms of the atomic fields, ψ_1 and ψ_2 , and the molecular fields, d_{12} and d_{22} , the EFT Lagrangian in a heteronuclear three-body system can be written as

$$\begin{aligned}
\mathcal{L} = & \psi_1^\dagger \left(i\partial_t + \frac{\nabla^2}{2m_1} \right) \psi_1 + \psi_2^\dagger \left(i\partial_t + \frac{\nabla^2}{2m_2} \right) \psi_2 \\
& - d_{12}^\dagger \left(i\partial_t + \frac{\nabla^2}{2(m_1 + m_2)} - \Delta_{12} \right) d_{12} + \Delta_{22} d_{22}^\dagger d_{22} \\
& - g_{12} \left(d_{12}^\dagger \psi_1 \psi_2 + \psi_1^\dagger \psi_2^\dagger d_{12} \right) - \frac{g_{22}}{\sqrt{2}} \left(d_{22}^\dagger \psi_2 \psi_2 + \psi_2^\dagger \psi_2^\dagger d_{22} \right) - h d_{12}^\dagger \psi_2^\dagger d_{12} \psi_2 \quad (1)
\end{aligned}$$

¹ The Feshbach resonances chosen in these specific experiments, however, also had a large Cs-Cs scattering length, a_{22} . Here we study systems with the scale hierarchy $r_0, a_{22} \ll a_{12}$.

where g_{12} and g_{22} are the two-body, and h , the three-body coupling constants. The masses of the particles of type 1 and type 2 are denoted with m_1 and m_2 , respectively. Since a_{22} is of natural size, the coupling constant between the identical atoms (that we will assume to be bosons), g_{22} , is treated perturbatively. The bare propagator of the d_{22} field then satisfies that

$$\frac{i}{\Delta_{22}} = i \frac{4\pi a_{22}}{m_2 g_{22}^2}. \quad (2)$$

The interspecies scattering length a_{12} is large such that atoms 1 and 2 form a two-body shallow virtual/bound molecular state. The propagator that represents this state is obtained by non-perturbative treatment of the coupling constant g_{12} . To simplify the introduction of a finite effective range, we employ a dynamical d_{12} field in Eq. (1). In order to preserve structure of the low-energy expansion and to extract the correction strictly linear in the effective range we expand this propagator as

$$\mathcal{D}_{12}(p_0, \mathbf{p}) = \mathcal{D}_{12}^{(0)}(p_0, \mathbf{p}) + \mathcal{D}_{12}^{(1)}(p_0, \mathbf{p}) + \dots, \quad (3)$$

and obtain the LO propagator,

$$i\mathcal{D}_{12}^{(0)}(p_0, \mathbf{p}) = -i \frac{2\pi}{\mu g_{12}^2} \frac{1}{-\gamma + \sqrt{-2\mu(p_0 - \frac{p^2}{2(m_1+m_2)})} - i\epsilon}, \quad (4)$$

and the NLO propagator,

$$i\mathcal{D}_{12}^{(1)}(p_0, \mathbf{p}) = -i \frac{\pi r_0}{\mu g_{12}^2} \frac{\gamma + \sqrt{-2\mu(p_0 - \frac{p^2}{2(m_1+m_2)})} - i\epsilon}{-\gamma + \sqrt{-2\mu(p_0 - \frac{p^2}{2(m_1+m_2)})} - i\epsilon}, \quad (5)$$

where $\mu = m_1 m_2 / (m_1 + m_2)$, $\mu_{AD} = m_2 (m_1 + m_2) / (m_1 + 2m_2)$, and γ denotes the interspecies binding momentum, which relates to a_{12} by $1/a_{12} = \gamma - r_0 \gamma^2 / 2$. At LO, we simply have $\gamma = 1/a_{12}$.

The atom-molecule (ψ_1 - d_{12}) scattering amplitude given at LO by the Lagrangian in Eq. (1) satisfies the Skorniakov–Ter-Martirosian (STM) equation depicted in Fig. 1,

$$\begin{aligned} \mathcal{A}_0(p, k; E) = & \frac{2\pi\gamma m_1}{\mu^2} \left[K(p, k; E) + \frac{H^{(0)}(\Lambda)}{\Lambda^2} \right] \\ & + \frac{m_1}{\pi\mu} \int_0^\Lambda dq q^2 \left[K(p, q; E) + \frac{H^{(0)}(\Lambda)}{\Lambda^2} \right] \frac{\mathcal{A}_0(q, k; E)}{-\gamma + \sqrt{-2\mu(E - \frac{q^2}{2\mu_{AD}})} - i\epsilon}. \end{aligned} \quad (6)$$

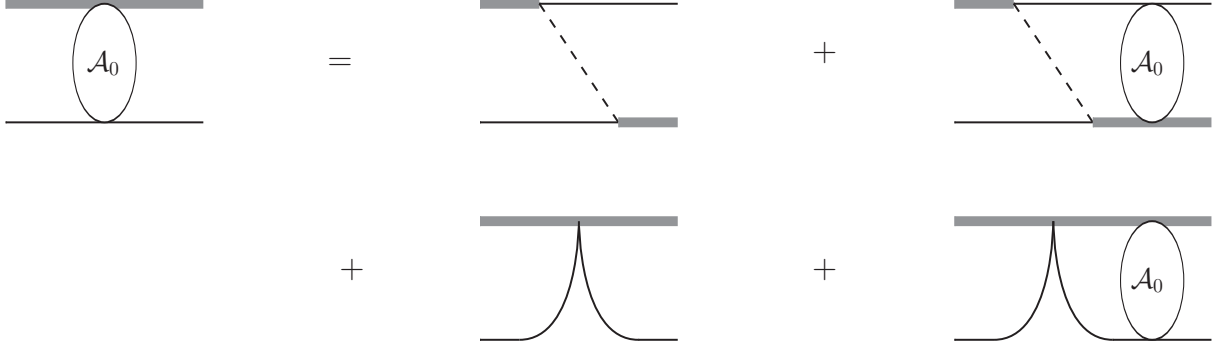


FIG. 1: The STM equation for the LO scattering amplitude. The dashed and the solid lines represent the propagators of atoms 1 and 2 respectively, and the thick gray line represents the dressed two-body propagator, $i\mathcal{D}_{12}^{(0)}$.

where p and k denote the relative momenta between the fields ψ_1 and d_{12} in the three-body center of mass frame. The kernel function K is defined as

$$K(p, q; E) = \frac{1}{2pq} \ln \frac{-2\mu E + p^2 + q^2 + 2pq/(1 + \delta) - i\epsilon}{-2\mu E + p^2 + q^2 - 2pq/(1 + \delta) - i\epsilon}, \quad (7)$$

where $\delta = m_1/m_2$ is the interspecies mass ratio and the coupling constant g_{12} has been eliminated by applying wave function renormalization to the external legs of the amplitude, with a LO renormalization factor $Z_{12} = 2\gamma/(\mu^2 g_{12}^2)$.

The leading order three-body force parameter, $H^{(0)}(\Lambda)$, that needs to be fixed by using one three-body datum as input, has the analytic form

$$H^{(0)}(\Lambda) = \frac{2c(\delta) \sin[s_0 \ln(\Lambda/\Lambda_*) + \arctan s_0]}{1 + \delta \sin[s_0 \ln(\Lambda/\Lambda_*) - \arctan s_0]}, \quad (8)$$

and is a log-periodic function of Λ . The three-body coupling $H^{(0)}$ is invariant under a discrete scaling transformation by a scaling factor $\lambda = \exp(\pi/s_0)$, where s_0 depends on the mass ratio δ (see Appendix A). The factor $c(\delta)$, which is obtained by matching Eq. (8) to the numerical value of $H^{(0)}(\Lambda)$, is required to render Eq. (6) independent of the cutoff Λ . It is shown as a function of δ in Fig. 2.

At NLO, the three-body amplitude \mathcal{A} can be modified as

$$\mathcal{A}(p, k; E) = (1 + \gamma r_0) \mathcal{A}_0(p, k; E) + \mathcal{A}_1(p, k; E). \quad (9)$$

As shown in Fig. 3, the NLO amplitude $\mathcal{A}_1(p, k; E)$ contains diagrams with one insertion of the NLO propagator, $i\mathcal{D}_{12}^{(1)}$, and those with one insertion of the bare propagator, i/Δ_{22} .

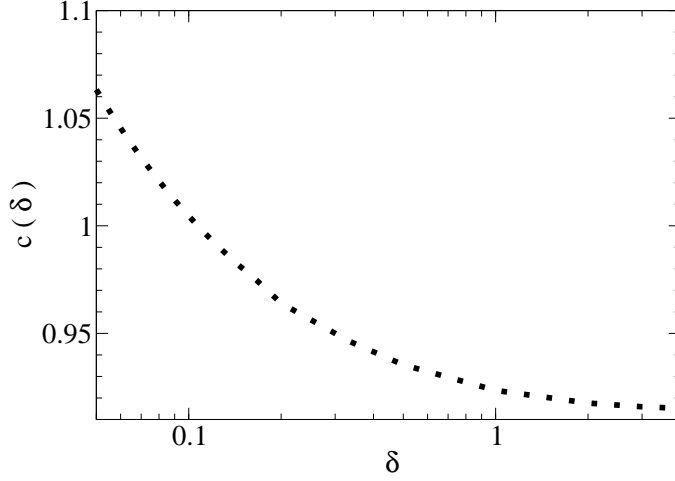


FIG. 2: The numerical prefactor c appearing in the LO three-body force $H_0(\Lambda)$ as a function of the mass ratio $\delta = m_1/m_2$.

To absorb their linear and logarithmic divergences, the diagrams with NLO three-body interactions are introduced. These Feynman diagrams can be evaluated to give

$$\begin{aligned}
\mathcal{A}_1(p, k; E) = & r_0 \frac{\mu}{4\pi^2\gamma} \int_0^\Lambda dq q^2 \frac{\gamma + \sqrt{-2\mu(E - \frac{q^2}{2\mu_{AD}}) - i\epsilon}}{-\gamma + \sqrt{-2\mu(E - \frac{q^2}{2\mu_{AD}}) - i\epsilon}} \mathcal{A}_0(p, q; E) \mathcal{A}_0(q, k; E) \\
& - a_{22} \frac{8\gamma m_2}{\mu^2} \int_0^\Lambda dq q^2 \mathcal{M}(p, q; E) \mathcal{M}(k, q; E) \\
& + \frac{H^{(1)}(\Lambda)}{\Lambda^2} \frac{2\pi\gamma m_1}{\mu^2} \left[1 + \frac{\mu}{2\pi^2\gamma} \int_0^\Lambda dq q^2 \frac{\mathcal{A}_0(p, q; E)}{-\gamma + \sqrt{-2\mu(E - \frac{q^2}{2\mu_{AD}}) - i\epsilon}} \right] \\
& \times \left[1 + \frac{\mu}{2\pi^2\gamma} \int_0^\Lambda dq q^2 \frac{\mathcal{A}_0(q, k; E)}{-\gamma + \sqrt{-2\mu(E - \frac{q^2}{2\mu_{AD}}) - i\epsilon}} \right], \quad (10)
\end{aligned}$$

where

$$\mathcal{M}(p, k; E) = G(p, k; E) + \frac{\mu}{2\pi^2\gamma} \int_0^\Lambda dq q^2 \frac{\mathcal{A}_0(p, q; E)}{-\gamma + \sqrt{-2\mu(E - \frac{q^2}{2\mu_{AD}}) - i\epsilon}} G(q, k; E), \quad (11)$$

with

$$G(p, k; E) = \frac{1}{2pk} \ln \frac{-m_2 E + p^2 + \frac{m_2}{2\mu} k^2 + pk - i\epsilon}{-m_2 E + p^2 + \frac{m_2}{2\mu} k^2 - pk - i\epsilon}. \quad (12)$$

The NLO three-body force has the form

$$H^{(1)}(\Lambda) = \Lambda[r_0 h_{10}(\Lambda) + a_{22} \bar{h}_{10}(\Lambda)] + \gamma[r_0 h_{11}(\Lambda) + a_{22} \bar{h}_{11}(\Lambda)] , \quad (13)$$

where h_{10} , h_{11} , \bar{h}_{10} and \bar{h}_{11} can be determined from experimental input. The γ -independent pieces of $H^{(1)}$, h_{10} and \bar{h}_{10} , can be fixed by renormalizing to the same observable that was used to reproduce the LO three-body parameter. However, as discussed later in Section IV, the γ -dependent parts of $H^{(1)}$ requires tuning h_{11} and \bar{h}_{11} to fix one additional three-body observable. In practice, one can work at a fixed value of Λ for these counterterms. However, it is useful to study their renormalization group evolution to ensure that the regularization and renormalization have been carried out correctly and consistently. We therefore analyze the renormalization-group flow of the coupling constants, $h_{10}(\Lambda)$, $h_{11}(\Lambda)$, $\bar{h}_{10}(\Lambda)$ and $\bar{h}_{11}(\Lambda)$ in the appendix.

III. NLO CORRECTIONS TO RECOMBINATION FEATURES

The specific observables that are considered to be signatures of Efimov physics are usually extracted from the so-called recombination rate in experiments with ultracold atomic gases. Below we discuss the NLO corrections to these features. Corresponding expressions for the case of three identical bosons were derived in Ref. [17].

A. Three-body binding energy

The LO scattering amplitude $\mathcal{A}_0(p, k; E)$ at a given γ has a series of discretized poles $E \rightarrow E_0^{(n)}(\gamma)$, where $E_0^{(n)}$ are the energies of the n th three-body bound states:

$$\mathcal{A}_0(p, k; E) = \frac{Z_0^{(n)}(p, k)}{E - E_0^{(n)}(\gamma)} + \mathcal{R}_0(p, k; E), \quad (14)$$

where $Z_0^{(n)}(p, k)$ is the residue of the pole and $\mathcal{R}_0(p, k; E)$ is the regular term around the pole expansion. Due to NLO corrections, the pole position, the residue and the regular term of $\mathcal{A}(p, k; E)$ are shifted by $E_1^{(n)}$, $Z_1^{(n)}$ and $\mathcal{R}_1(p, k; E)$ respectively, i.e.

$$\mathcal{A}(p, k; E) = \frac{Z_0^{(n)}(p, k) + Z_1^{(n)}(p, k)}{E - E_0^{(n)}(\gamma) - E_1^{(n)}(\gamma)} + \mathcal{R}_0(p, k; E) + \mathcal{R}_1(p, k; E), \quad (15)$$

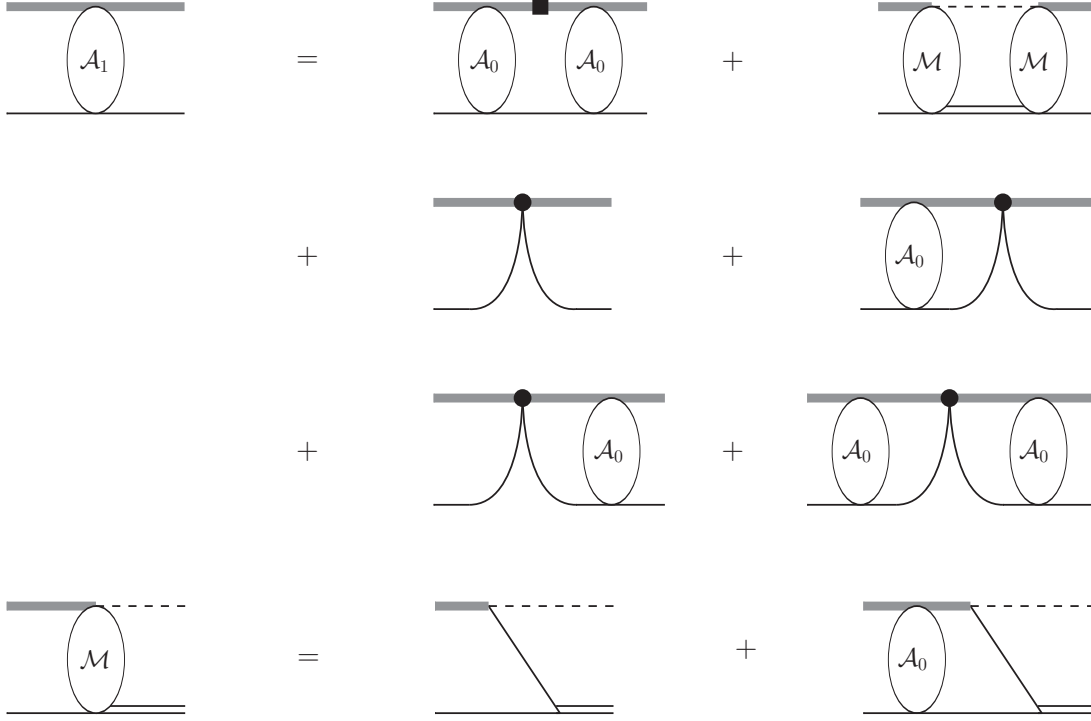


FIG. 3: The upper equation shows the NLO scattering amplitude, $i\mathcal{A}_1$. The thick gray line with a black square represents the NLO dressed propagator, $i\mathcal{D}_{12}^{(1)}$, the double line represents the bare propagator of the d_{22} field, and the three-atom vertex with circle represents the NLO three-body force. The lower equation defines the coupled-channel amplitude, which, up to constant factors, is equal to \mathcal{M} defined in Eq. (11).

Matching terms linear in r_0 and a_{22} , we obtain

$$E_1^{(n)}(\gamma) = \frac{\lim_{E \rightarrow E_0^{(n)}} [E - E_0^{(n)}(\gamma)]^2 \mathcal{A}_1(p, k; E)}{\lim_{E \rightarrow E_0^{(n)}} [E - E_0^{(n)}(\gamma)] \mathcal{A}_0(p, k; E)}. \quad (16)$$

B. Three-body recombination rate

If $a_{12} > 0$, three free atoms can recombine into a shallow two-atom bound state and a residual atom. The energy released due to the formation of the bound state is now converted to kinetic energy and all three atoms leave the trap. The Feynman diagrams that contribute to the amplitude for this process, iT_{rec} , are shown in Fig. 4.

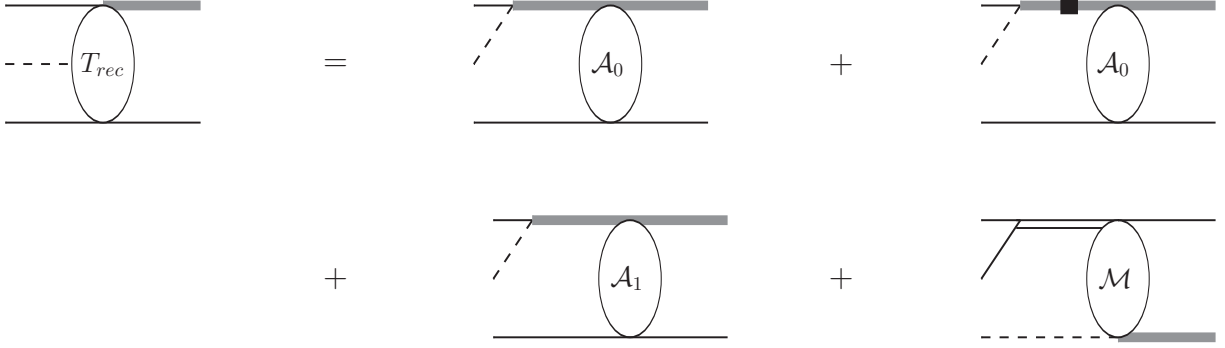


FIG. 4: The amplitude for the recombination of free atoms into shallow two-atom bound state and a residual atom. The first term on the right hand side is the LO amplitude and the rest are NLO corrections.

The rate of change of the number densities of the atoms, $n_{1,2}$ due to this recombination process is

$$\frac{dn_2}{dt} = 2 \frac{dn_1}{dt} = -2\alpha n_1 n_2^2, \quad (17)$$

where, up to NLO, the rate constant, α_s is given by

$$\alpha_s = 4 \sqrt{\frac{\mu_{AD}^3}{\mu}} \frac{1}{\gamma^2} \left| \mathcal{A}(0, \sqrt{\frac{\mu_{AD}}{\mu}} \gamma; 0) + a_{22} 4\pi \frac{\gamma^2}{\mu} \mathcal{M}(\sqrt{\frac{\mu_{AD}}{\mu}} \gamma, 0; 0) \right|^2. \quad (18)$$

At LO, the rate constant has a minimum at γ_0 given by

$$\mathcal{A}_0(0, \sqrt{\frac{\mu_{AD}}{\mu}} \gamma_0; 0) = 0. \quad (19)$$

The NLO corrections shift the position of the recombination minimum to $\gamma_0 + \Delta\gamma$, where $\Delta\gamma$ is given by the condition

$$\frac{d}{d\gamma} \mathcal{A}_0(0, \sqrt{\frac{\mu_{AD}}{\mu}} \gamma; 0) \Big|_{\gamma=\gamma_0} \Delta\gamma + \mathcal{A}_1(0, \sqrt{\frac{\mu_{AD}}{\mu}} \gamma_0; 0) + a_{22} 4\pi \frac{\gamma^2}{\mu} \mathcal{M}(\sqrt{\frac{\mu_{AD}}{\mu}} \gamma_0, 0; 0) = 0. \quad (20)$$

C. Atom-molecule resonance

The atom-molecule relaxation rate has a resonance when the a three-body bound state crosses the atom-dimer threshold, i.e. when the three-body bound state energy coincides with the two-body bound-state energy. The NLO shift in the resonance position, $\Delta\gamma_*$, is given by the condition

$$\Delta\gamma_* \lim_{\gamma \rightarrow \gamma_*} (\gamma - \gamma_*) \mathcal{A}_0(0, 0; \frac{-\gamma^2}{2\mu}) = \lim_{\gamma \rightarrow \gamma_*} (\gamma - \gamma_*)^2 \mathcal{A}_1(0, 0; \frac{-\gamma^2}{2\mu}) \quad (21)$$

| System | δ | λ | θ_0 | θ_* | θ_- |
|-------------------------|------------------------|---------------------|------------|------------------------|------------|
| ${}^6\text{Li-Cs-Cs}$ | 4.511×10^{-2} | 4.865 | 0.6114 | 3.388×10^{-2} | -1.349 |
| ${}^7\text{Li-Cs-Cs}$ | 5.263×10^{-2} | 5.465 | 0.5887 | 3.392×10^{-2} | -1.376 |
| ${}^6\text{Li-Rb-Rb}$ | 6.897×10^{-2} | 6.835 | 0.5492 | 3.367×10^{-2} | -1.436 |
| ${}^7\text{Li-Rb-Rb}$ | 8.046×10^{-2} | 7.864 | 0.5266 | 3.328×10^{-2} | -1.477 |
| ${}^{40}\text{K-Rb-Rb}$ | 0.4598 | 1.227×10^2 | 0.2194 | 1.014×10^{-2} | -2.430 |
| ${}^{41}\text{K-Rb-Rb}$ | 0.4713 | 1.310×10^2 | 0.2142 | 9.705×10^{-3} | -2.451 |

TABLE I: LO universal Efimov parameters for different heteronuclear systems.

where γ_* is the resonance position at LO.

D. Three-atom resonance

Three-atom resonances occur when zero-energy three-body bound states form, and result in maxima in the three-atom recombination rate. At LO, this happens at γ equals $\gamma_- < 0$ when the Efimov curve crosses the three-atom threshold. The NLO correction to the resonance position is given by

$$\Delta\gamma_- = -\frac{E_1^{(n)}(\gamma_-)}{\left.\frac{dE_0^{(n)}(\gamma)}{d\gamma}\right|_{\gamma=\gamma_-}}. \quad (22)$$

IV. UNIVERSAL RELATIONS AND RENORMALIZATION GROUP IMPROVEMENT

We use a_i , where i runs over 0, * and -, to label the values of a_{12} associated with the signatures of the Efimov effect. At LO, for which $a_i = 1/\gamma_i$, the universal relations between the various three-body observables can be summarized as

$$a_i^{(n)} = \lambda^n \theta_i \kappa_*^{-1}, \quad (23)$$

where κ_* is the binding momentum of the 0th state at the unitary limit $\kappa_* \equiv \sqrt{2\mu|E_0^{(0)}(0)|}$. The values of λ and θ_i for various systems are listed in Table I.

At NLO, we can write similar relations that express a desired recombination feature as a

| System | $\sigma = 2(J_0 - J_-)$ | $J_* - J_0$ | $\bar{\sigma} = 2(Y_0 - Y_-)$ | $Y_* - Y_0$ |
|-------------------------|-------------------------|-------------|-------------------------------|-------------|
| ${}^6\text{Li-Cs-Cs}$ | 0.693 | 0.840 | 0.141 | 0.680 |
| ${}^7\text{Li-Cs-Cs}$ | 0.743 | 0.828 | 0.204 | 0.821 |
| ${}^6\text{Li-Rb-Rb}$ | 0.840 | 0.820 | 0.367 | 1.11 |
| ${}^7\text{Li-Rb-Rb}$ | 0.904 | 0.823 | 0.502 | 1.30 |
| ${}^{40}\text{K-Rb-Rb}$ | 2.74 | 1.52 | 12.1 | 8.74 |
| ${}^{41}\text{K-Rb-Rb}$ | 2.80 | 1.54 | 12.7 | 9.07 |

TABLE II: NLO universal Efimov parameters for different heteronuclear systems.

sum of the LO universal relation and shifts linear in r_0 and a_{22} ,

$$a_i^{(n)} = \lambda^n \theta_i \kappa_*^{-1} + (J_i - n\sigma)r_0 + (Y_i - n\bar{\sigma})a_{22}, \quad (24)$$

where J_i and Y_i are numbers that depend on the renormalization condition chosen at NLO and σ and $\bar{\sigma}$ are universal numbers that depends only on the mass ratio in the heteronuclear system. The quantities J_i and Y_i are not universal, however, their differences, $(J_i - J_j)$ and $(Y_i - Y_j)$, are universal. To explicitly show the correlation between any three Efimov features in terms of universal numbers only, we rewrite Eq. (24) as

$$a_j^{(m)} = a_i^{(n)} + \left(\lambda^{m-l} \frac{\theta_j}{\theta_k} - \lambda^{n-l} \frac{\theta_i}{\theta_k} \right) a_k^{(l)} + [(J_j - J_i) - (m - n)\sigma] r_0 + [(Y_j - Y_i) - (m - n)\bar{\sigma}] a_{22}, \quad (25)$$

which can be used to make predictions for all j and m using any two Efimov features, $a_i^{(n)}$ and $a_k^{(l)}$, as inputs. The values of the NLO universal numbers for different systems are listed in Table II. Empirically, we find further correlations between these universal numbers. We obtain $J_0 - J_- = \sigma/2$ and $Y_0 - Y_- = \bar{\sigma}/2$ for all values of the mass ratio δ .

The expressions for the three-body counterterms derived in the appendix are very similar in structure to the ones that have been derived for three identical bosons in Ref. [17]. In particular, the subleading three-body counterterms h_{11} and \bar{h}_{11} contain terms that indicate a logarithmic violation of the leading order discrete scaling invariance. We can separate out these terms by writing the full three-body force as

$$H(\Lambda) = H_0(\Lambda) + h_{10}(\Lambda)\Lambda r_0 + \bar{h}_{10}(\Lambda)\Lambda a_{22} + [\nu H'(\Lambda) \ln(\Lambda/Q_*) + \xi(\Lambda)] \gamma r_0 + [\bar{\nu} H'(\Lambda) \ln(\Lambda/Q_*) + \bar{\xi}(\Lambda)] \gamma a_{22}, \quad (26)$$

where Q_* is the three-body parameter for the NLO renormalization, which is determined by the additional three-body observable reproduced at this order. $H'(\Lambda)$ denotes the logarithmic derivative of the LO three-body force, *i.e.*, $H'(\Lambda) \equiv dH(\Lambda)/(\Lambda d\Lambda)$. The dimensionless ratios ν and $\bar{\nu}$ are defined in the appendix. The redefined counterterms $\xi(\Lambda)$ and $\bar{\xi}(\Lambda)$ in the above equation are periodic functions of $\ln \Lambda$. Their explicit expressions are not necessary for deriving the renormalization-group flow equation.

The term proportional to $\ln \Lambda/Q_*$ can be absorbed into H_0 by defining a *running* Efimov parameter

$$\bar{\kappa}_* = (Q_*/\kappa_*)^{-\nu\gamma r_0 - \bar{\nu}\gamma a_{22}} \kappa_* . \quad (27)$$

Now we can write down renormalization group improved universal relations by elimination κ_* in Eq. (24) in favor of the running Efimov parameter $\bar{\kappa}_*$ defined in Eq. (27)

$$a_{i,n} = \lambda^n \theta_i (\lambda^n |\theta_i|)^{-(\nu r_0 + \bar{\nu} a_{22})\kappa_*/(\lambda^n \theta_i)} \kappa_*^{-1} + r_0 \tilde{J}_i + a_{22} \tilde{Y}_i . \quad (28)$$

Matching Eq. (24) and Eq. (28) yields $\sigma = \nu \ln \lambda$ and $\bar{\sigma} = \bar{\nu} \ln \lambda$ and

$$\begin{aligned} \tilde{J}_i &= J_i + \nu \ln |\theta_i| \\ \tilde{Y}_i &= Y_i + \bar{\nu} \ln |\theta_i| \end{aligned} \quad (29)$$

The differences between the coefficients \tilde{J}_j are universal numbers and so are differences between the coefficients \tilde{Y}_i .

In Refs. [19, 20] it was shown that a simple modification of analytic expressions for zero-range observables can account in a simple manner for a finite range corrections. In Ref. [18] it was shown that the underlying reason for this simple approach is the slow logarithmic running of the modified Efimov parameter shown above in Eq. (27). In the heteronuclear system, we can infer from the renormalization-group-improved universal relations above that the same strategy can account for higher order corrections by modifying the analytic results presented in Ref. [12]. This will facilitate a simple inclusion of the effects of deeply bound two-body states that have energies larger than $1/(\mu r_0^2)$.

For the recombination rate at positive scattering length, the authors of Ref. [12] found

$$\alpha_s = C(\delta) \frac{128\pi^2(4\pi - 3\sqrt{3}) [\sin^2(s_0 \ln(a_{12}/a_+)) + \sinh^2 \eta_*] a_{12}^4}{\sinh^2(\pi s_0 + \eta_*) + \cos^2(s_0 \ln(a_{12}/a_+)) m_1} , \quad (30)$$

where $C(\delta)$ is a mass dependent coefficient that has been calculated in Ref. [12]. Following the prescription laid out in Refs. [19, 20], we replace the a_{12}^4 factor in Eq. (30) with γ^{-4} and

additionally introduce the parameter Γ that shifts the three-body parameter according to $a_i^{-1} \rightarrow a_i^{-1} + \Gamma/a_{12}$. The parameter Γ , which accounts for the corrections due to r_0 as well as those due to a_{22} , is different for each system and each observable a_i and can be fit to data. Using these substitutions, we obtain

$$\alpha_s = C(\delta) \frac{128\pi^2(4\pi - 3\sqrt{3}) [\sin^2(s_0 \ln(a_{12}/a_+ + \Gamma)) + \sinh^2 \eta_*]}{\sinh^2(\pi s_0 + \eta_*) + \cos^2(s_0 \ln(a_{12}/a_+ + \Gamma))} \frac{1}{\gamma^4 m_1} \quad (31)$$

Modifying the corresponding equation given in Ref. [12] for the rate of recombination into deeply bound two-body states at positive scattering length leads to

$$\alpha_d = C(\delta) \frac{\coth(\pi s_0) \cosh(\eta_*) \sinh(\eta_*)}{\sinh^2(\pi s_0 + \eta_*) + \cos^2(s_0 \ln(a_{12}/a_+ + \Gamma))} \frac{1}{\gamma^4 m_1}, \quad (32)$$

where Γ needs to have the same value as in Eq. (31). The total recombination rate for positive scattering length is then given as the sum of recombination into shallow and deeply bound two-body states,

$$\alpha = \alpha_s + \alpha_d. \quad (33)$$

The same conjecture can be made for negative scattering length and the analytic expression derived in Ref. [12] for the rate of recombination into deeply bound two-body states leads to

$$\alpha_d = \frac{C(\delta)}{2} \frac{128\pi^2(4\pi - 3\sqrt{3}) \coth(\pi s_0) \sin(2\eta_*)}{\sin^2(s_0 \log(a_{12}/a_- + \Gamma')) + \sinh^2(\eta_*)} \frac{1}{\gamma^4 m_1}. \quad (34)$$

where we used the parameter Γ' to emphasize that it is different from the parameter Γ used in the previous equations.

V. SUMMARY

In this work we have calculated recombination features of the heteronuclear three-body system at NLO in the short-range EFT expansion. Specifically, we have considered systems in which the interspecies scattering length is large compared to the van der Waals length scale, and the effective range and the intraspecies scattering length are of comparable size. At leading order in the EFT expansion, only the interspecies scattering length and one three-body observable are required within this approach for predictions. At NLO, a second three-body observable is required in addition to the effective range and the intraspecies scattering length. Our results give rise to universal relations that can be used to predict

recombination features as a function of two-body scattering parameters and two three-body observables. The parameters in these relations are universal and depend only on the mass ratio in the heteronuclear system. We have explicitly calculated these universal numbers for a number of physical systems of interest. In particular, the ${}^6\text{Li-Cs-Cs}$ seems to be well suited to obtain experimental numbers to test our universal relations. Alternatively, these relations could be tested using few-body calculations with microscopic interactions as was done in Ref. [18].

An extension of this research is to account for range corrections when both the scattering lengths in the heteronuclear system become simultaneously large. Work along these lines is under development. However, generally, we expect universal relations that account for finite range effects in other systems to look very similar to the ones presented here. The most general case of course would be to consider a system of three distinguishable particles with three different scattering lengths.

A further important extension of our work is to apply this approach to study systems at finite temperature in order to understand the influence of the temperature effects on the positions of recombination features. For example, it was shown in Ref. [21] that finite range effects lead to measurable temperature dependence of the recombination features. How to include the effect of recombination into deeply bound two-body states at next-to-leading order in effective field theory is also an open question.

Acknowledgments

This work was supported by the Office of Nuclear Physics, U.S. Department of Energy under Contract No. DE-AC05-00OR22725, the National Science Foundation under Grant No. PHY-1516077 and by the Natural Sciences and Engineering Research Council (NSERC), and the National Research Council of Canada. LP thanks the ExtreMe Matter Institute EMMI at the GSI Helmholtz Centre for Heavy Ion Research for support and the Institute of Nuclear Physics at the TU Darmstadt for its hospitality during the completion of this work.

Appendix A: Renormalization group evolution of the NLO three-body interaction

Following Ref. [17], we can derive the asymptotic expression for the LO amplitude $\mathcal{A}_0(p, k; E)$ for $p \gg k$, $p \gg \sqrt{-2\mu E}$,

$$\mathcal{A}_0(p, k; E) \sim \tilde{\mathcal{A}}_0(p) = \frac{z_0(p)}{p} + \gamma \frac{z_1(p)}{p^2} + \dots, \quad (\text{A1})$$

where the log-periodic functions $z_{0,1}$ are

$$z_0(p) = \sin \left(s_0 \ln \frac{p}{\Lambda_*} \right), \quad (\text{A2})$$

and

$$z_1(p) = \frac{1}{\cos \phi} |C_{-1}| \sin \left(s_0 \ln \frac{p}{\Lambda_*} + \arg C_{-1} \right). \quad (\text{A3})$$

Here the constant s_0 and C_{-1} are solved in a transcendental equation which satisfies that

$$\mathcal{I}(is_0) = 1, \quad (\text{A4})$$

and

$$C_{-1} = \frac{\mathcal{I}(is_0 - 1)}{1 - \mathcal{I}(is_0 - 1)}. \quad (\text{A5})$$

The function $\mathcal{I}(s)$ is defined as

$$\mathcal{I}(s) = \frac{2 \sin(\phi s)}{s \cos \left(\frac{\pi s}{2} \right) \sin(2\phi)}, \quad (\text{A6})$$

where $\phi = \arcsin(1/(1 + \delta))$.

Using Eq. (A1) in Eq. (11), we can find a similar asymptotic form of $\mathcal{M}(p, k; E)$ at $p \gg k$ and $p \gg \sqrt{-2\mu E}$,

$$\mathcal{M}(p, k; E) \sim \tilde{\mathcal{M}}(p) = \frac{\sqrt{\mu\mu_{AD}}}{2\pi s_0 \gamma} \frac{\sinh(s_0 \beta)}{\cosh\left(\frac{\pi s_0}{2}\right)} \left[\frac{1}{p} z_0 \left(\frac{\rho p}{2} \right) + \frac{2\gamma}{\rho p^2} \bar{z}_1 \left(\frac{\rho p}{2} \right) + \dots \right], \quad (\text{A7})$$

where $\rho = \sqrt{2m_2/\mu}$ and $\beta = \arcsin(1/\rho)$, and

$$\bar{z}_1(p) = \frac{1}{\cos \phi} |D_{-1}| \sin \left(s_0 \ln \frac{p}{\Lambda_*} + \arg D_{-1} \right), \quad (\text{A8})$$

with

$$D_{-1} = \frac{s_0}{is_0 - 1} \frac{\sin(\beta[is_0 - 1])}{\sinh(s_0 \beta)} \frac{\cosh\left(\frac{\pi s_0}{2}\right)}{\cos\left(\frac{\pi}{2}[is_0 - 1]\right)} (1 + C_{-1}). \quad (\text{A9})$$

Using Eqs. (A1) and (A7) the ultraviolet behavior of the integrals in Eq. (10) can be analyzed. There are linear and logarithmic divergences proportional to both r_0 and a_{22}

which can be removed by appropriate choices for the renormalization group evolution of the counter terms $h_{10}(\Lambda)$, $h_{11}(\Lambda)$, $\bar{h}_{10}(\Lambda)$ and $\bar{h}_{11}(\Lambda)$. The expressions for the running of $h_{10}(\Lambda)$ and $\bar{h}_{10}(\Lambda)$ are,

$$h_{10}(\Lambda) = -\frac{\pi(1+s_0^2)}{8} \sin(2\phi) \cos\phi \frac{(1+4s_0^2)^{\frac{1}{2}} - \cos\left(2s_0 \ln \frac{\Lambda}{\Lambda_*} - \arctan(2s_0)\right)}{(1+4s_0^2)^{\frac{1}{2}} \sin^2\left(s_0 \ln \frac{\Lambda}{\Lambda_*} - \arctan s_0\right)} \quad (\text{A10})$$

and

$$\bar{h}_{10}(\Lambda) = \frac{2\pi}{\delta} \frac{1+s_0^2}{s_0^2} \frac{\sinh^2(s_0\beta)}{\cosh^2\left(\frac{\pi s_0}{2}\right)} \frac{(1+4s_0^2)^{\frac{1}{2}} - \cos\left(2s_0 \ln \frac{\rho\Lambda}{2\Lambda_*} - \arctan(2s_0)\right)}{(1+4s_0^2)^{\frac{1}{2}} \sin^2\left(s_0 \ln \frac{\Lambda}{\Lambda_*} - \arctan s_0\right)}. \quad (\text{A11})$$

The value of Λ_* in these equations is determined by the LO renormalization condition and can be obtained from Eq. (8). Eqs. (A10) and (A11) are, therefore, predictive.

Similarly, the expressions for the running of $h_{11}(\Lambda)$ and $\bar{h}_{11}(\Lambda)$ are,

$$h_{11}(\Lambda) = -d_K(\delta) \frac{\pi(1+s_0^2)}{4} \sin(2\phi) \frac{1+|C_{-1}| \cos(\arg C_{-1})}{\sin^2\left(s_0 \ln \frac{\Lambda}{\Lambda_*} - \arctan s_0\right)} \ln \frac{\Lambda}{Q_*} + \xi(\Lambda), \quad (\text{A12})$$

and

$$\begin{aligned} \bar{h}_{11}(\Lambda) &= \bar{d}_K(\delta) \frac{8\pi}{\delta \cos\phi} \frac{1+s_0^2}{s_0^2} \frac{\sinh^2(s_0\beta)}{\cosh^2\left(\frac{\pi s_0}{2}\right)} \frac{1}{\rho} \frac{|D_{-1}| \cos(\arg D_{-1})}{\sin^2\left(s_0 \ln \frac{\Lambda}{\Lambda_*} - \arctan s_0\right)} \ln \frac{\Lambda}{Q_*} \\ &+ \bar{\xi}(\Lambda), \end{aligned} \quad (\text{A13})$$

where $\xi(\Lambda)$ and $\bar{\xi}(\Lambda)$ are periodic functions of $\ln \Lambda$, and $d_K(\delta)$ and $\bar{d}_K(\delta)$ are numerical constants whose values are close to 1. To make the arguments of the logarithms dimensionless, we use the momentum scale Q_* . The constants $d_K(\delta)$ and $\bar{d}_K(\delta)$, which are independent of the choice of Q_* , can be determined by numerically evaluating the running of $h_{11}(\Lambda)$ and $\bar{h}_{11}(\Lambda)$ while maintaining the renormalization group invariance of physical observables, and then demanding that Eqs. (A12) and (A13) yield log-periodic values for the functions $\xi(\Lambda)$ and $\bar{\xi}(\Lambda)$. To illustrate, we plot these functions for the ${}^6\text{Li-Cs-Cs}$ system for a particular choice of renormalization conditions in Fig. 5. We find numerically that $d_K(\delta) = \bar{d}_K(\delta)$ for all systems. This equality stems from the fact that the regularization and the renormalization schemes for both the counterterms h_{11} and \bar{h}_{11} are the same.

Eq. (26) can now be obtained from Eqs. (8), (A12) and (A13) by defining

$$\nu = \frac{\pi(1+s_0^2)^2}{8s_0^2} \cos\phi [1+|C_{-1}| \cos(\arg C_{-1})] \frac{d_K(\delta)}{c(\delta)}, \quad (\text{A14})$$

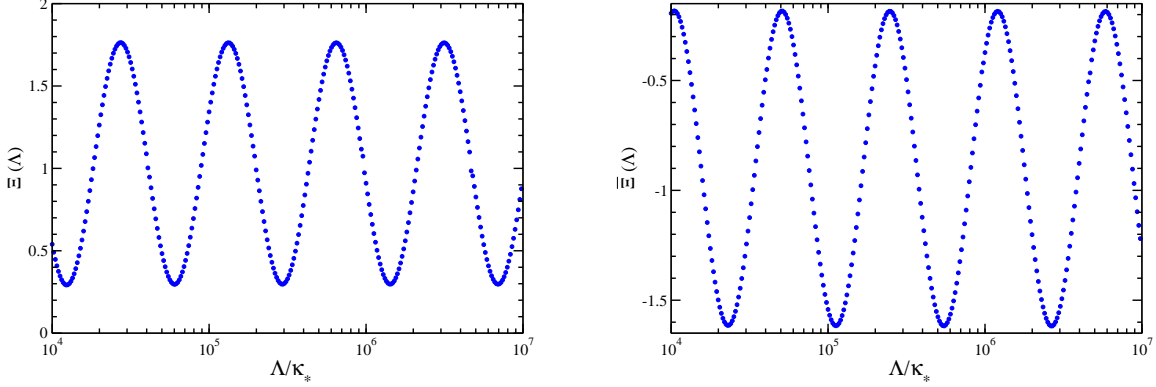


FIG. 5: The functions $\Xi(\Lambda) \equiv \xi(\Lambda) \sin^2 \left(s_0 \ln \frac{\Lambda}{\Lambda_*} - \arctan s_0 \right)$ and $\bar{\Xi} \equiv \bar{\xi}(\Lambda) \sin^2 \left(s_0 \ln \frac{\Lambda}{\Lambda_*} - \arctan s_0 \right)$ for the ${}^6\text{Li-Cs-Cs}$ system. The renormalization conditions were $E_1^{(0)}(0) = 0$ and $\Delta\gamma_0 = 0$. Q_* was chosen to be equal to κ_* . Periodicity of these functions in $\ln \Lambda$ could be obtained by requiring both d_R and \bar{d}_R to have the value 0.981.

and

$$\bar{\nu} = -\frac{4\pi}{\delta \sin(2\phi)} \frac{(1 + s_0^2)^2}{s_0^4} \frac{\sinh^2(s_0\beta)}{\cosh^2\left(\frac{\pi s_0}{2}\right)} \frac{1}{\rho} |D_{-1}| \cos(\arg D_{-1}) \frac{\bar{d}_K(\delta)}{c(\delta)}. \quad (\text{A15})$$

-
- [1] V. Efimov, Phys. Lett. **33B**, 563 (1970).
- [2] E. Braaten and H. W. Hammer, Phys. Rept. **428**, 259 (2006), arXiv:cond-mat/0410417.
- [3] T. Kraemer, M. Mark, P. Waldburger, J. G. Danzl, C. Chin, B. Engeser, A. D. Lange, K. Pilch, A. Jaakkola, H.-C. Nägerl, and R. Grimm, Nature **440**, 315 (2006).
- [4] N. Gross, Z. Shotan, S. Kokkelmans, and L. Khaykovich, Phys. Rev. Lett. **103**, 163202 (2009), arXiv:0906.4731.
- [5] S. E. Pollack, D. Dries, and R. G. Hulet, Science **326**, 1683 (2009), arXiv:0911.0893.
- [6] N. Gross, Z. Shotan, S. Kokkelmans, and L. Khaykovich, Phys. Rev. Lett. **105**, 103203 (2010), arXiv:1003.4891.
- [7] G. Barontini, C. Weber, F. Rabatti, J. Catani, G. Thalhammer, M. Inguscio, and F. Minardi, Phys. Rev. Lett. **103**, 043201 (2009), arXiv:0901.4584; Erratum: Ibid **104**, 059901 (2010).
- [8] S.-K. Tung, K. Jiménez-García, J. Johansen, C. V. Parker, and C. Chin, Phys. Rev. Lett. **113**, 240402 (2014), arXiv:1402.5943.

- [9] R. Pires, J. Ulmanis, S. Häfner, M. Repp, A. Arias, E. D. Kuhnle, and M. Weidemüller, *Phys. Rev. Lett.* **112**, 250404 (2014), arXiv:1403.7246.
- [10] L. Platter, *Few Body Syst.* **46**, 139 (2009), arXiv:0904.2227.
- [11] C. Ji, *International Journal of Modern Physics E* **25**, 1641003 (2016), arXiv:1512.06114.
- [12] K. Helfrich, H. W. Hammer, and D. S. Petrov, *Phys. Rev.* **A81**, 042715 (2010), arXiv:1001.4371.
- [13] N. T. Zinner and N. G. Nygaard, *Few-Body Systems* **56**, 125 (2015), arXiv:1403.0759.
- [14] Y. Wang, J. Wang, J. P. D’Incao, and C. H. Greene, *Phys. Rev. Lett.* **109**, 243201 (2012);
Erratum: *Ibid* **115**, 069901 (2015).
- [15] H. W. Hammer and T. Mehen, *Phys. Lett. B* **516**, 353 (2001), arXiv:nucl-th/0105072.
- [16] C. Ji, D. Phillips, and L. Platter, *Europhys. Lett.* **92**, 13003 (2010), arXiv:1005.1990.
- [17] C. Ji, D. R. Phillips, and L. Platter, *Annals Phys.* **327**, 1803 (2012), arXiv:1106.3837.
- [18] C. Ji, E. Braaten, D. R. Phillips, and L. Platter, *Phys. Rev.* **A92**, 030702(R) (2015), arXiv:1506.02334.
- [19] A. Kievsky and M. Gattobigio, *Phys. Rev.* **A87**, 052719 (2013), arXiv:1212.3457.
- [20] E. Garrido, M. Gattobigio, and A. Kievsky, *Phys. Rev. A* **88**, 032701 (2013), arXiv:1306.1711.
- [21] B. Huang, L. A. Sidorenkov, and R. Grimm, *Phys. Rev. A* **91**, 063622 (2015), arXiv:1504.05360.